Singaporean Journal of Scientific Research(SJSR)
Special Issue - Journal of Selected Areas in Microelectronics (JSAM)
Vol.8.No.2 2016 Pp.01- 11
available at :www.iaaet.org/sjsr
Paper Received : 08-04-2016
Paper Accepted: 25-04-2016
Paper Reviewed by: 1.Prof. Cheng Yu 2. Dr.G. Ramesh
Editor : Dr. Chu Lio

ANN BASED IMAGE CLASSIFIER FOR PANCREATIC CANCER DETECTION

M. Arunkumar [1], Dr. A. Murthi [2],
PG Student[1], Associate Professor[2],
Dept. of Electrical and Electronics Engineering,
Government College of Engineering, Salem
Tamil Nadu, India

ABSTRACT

The pancreatic cancer is having the rank of twelve among the common cancers in the world. As per the Cancer Facts and Figures Report 2015 released by the American Cancer Society, the estimated pancreatic cancer deaths for the year 2015 in the United States of America are around 40,560 persons. In India, around 17,000 persons are suffering from pancreatic cancer. Most of the pancreatic cancer deaths occur due to late detection of the disease where cancer spreads throughout the pancreas and to the nearby organ like the liver. The symptoms of this disease are vague, and so it is not helpful to detect the disease at the early stage. A new method is developed in this work for detecting this disease at the early stage. This method uses Artificial Neural Network (ANN) based image classifier in MATLAB software to detect pancreatic cancer from the Positron Emission Tomography (PET) scan images of the diagnosed persons. The developed method provides higher accuracy in detecting pancreatic cancer when compared with the existing method.

Keywords *– PET scan image, Image De-noising, Image Segmentation, Gray Level Co-occurrence Matrix (GLCM), and Artificial Neural Network (ANN) Classifier*

I. INTRODUCTION

Pancreatic cancer is one of the leading causes of the cancer deaths in the world. It is having the rank of twelve among the common cancers in the world [1]. As per the "Cancer Facts and Figures Report 2015" of the American Cancer Society, the estimated pancreatic cancer

deaths for the year 2015 in the United States of America are around 40,560 persons [2]. In India, the pancreatic cancer cases are about 17,000 patients [3]. The existing diagnosis methods are not capable of detecting this disease at the early stage as most of them depend on the symptoms of the disease which are vague. The cancer cells are capable of growing fast, and the late detection of cancer causes it to spread throughout the pancreas and to the nearby organs. Therefore, the early stage detection of pancreatic cancer requires the development of new diagnosis method. The developed method in this work uses ANN based image classifier in MATLAB software to detect pancreatic cancer at the early stage using the PET scan images of the diagnosed persons.

Jeenal Shah, Sunil Surve, Varsha Turkar performed the first experimental work on pancreatic cancer detection using image processing from the Computed Tomography (CT) scan images of the pancreatic cancer patients obtained from the internet [5]. They used minimum distance classifier algorithm and obtained accuracy of 65.26%. Minakshi Sharma and Sourabh Mukherjee performed the brain tumor detection using SVM classifier and achieved the accuracy of 97.9% [11]. Alireza Osareh and Bita Shadgar used SVM classifier in detecting Breast cancer and got an accuracy of 98.80% [14]. The remaining sections of this paper are arranged as follows. The section.3 discuss about PET scan images. The section.4 describes about Gray scale images. The section.5 discuss about the noise removal of the image. The section.6 represents the image segmentation by image threshold. The section.7 deals with the feature extraction by GLCM. The section.8 describes about the ANN-based image classification, and the section.9 provides the experimental results and discussions.

II. KEY CONTRIBUTION

In this work, ANN based image classifier is developed in the MATLAB software (MATLAB R2013a) to detect pancreatic cancer from the PET scan images of the diagnosed persons. The Fig.1 shows the algorithmic steps of the program. In the first step, the program uses the PET scan images of the diagnosed persons as its input data. In the second step, gray scale images are generated from color images. In the third step, gray scale images were de-noised using the median filter. In the fourth step, image threshold segments the cancer region. The segmented images are the output images of the program. In the fifth step, the program extracts the features of the segmented image using GLCM. In the sixth step, ANN classifier classifies the diagnosed images into either normal or cancer images using the extracted features.

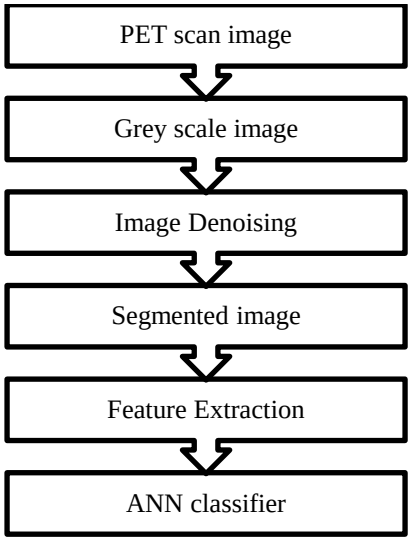

Fig.1 Pictorial representation of the various algorithmic steps of the program

III. PET SCAN IMAGE

The cells in the human body consume glucose as its energy for the metabolism. The glucose consumption level varies for normal and cancer cells. The cancer cells consume

more glucose than the normal cells. A PET scan is a type of nuclear imaging technique in which the patient receives a small amount of radioactive substance called Fluorodeoxyglucose (FDG) into his body through injection [4]. The cancer cells consume more amount of FDG than the normal cells. A scanner captures this change in the FDG consumption and develops the PET scan image. In this image, the cancer cells which consume more amount of FDG appear brighter when compared with the normal cells. The PET scan image has the advantage of capturing even a small-sized tumor of the pancreas which the CT or MRI or Abdominal Ultrasonography scans fails to capture. Therefore, PET scan detects pancreatic cancer at the early stage by capturing the tumor at the beginning stage (i.e., small-sized tumor). This program classified the fifty PET scan images of different persons collected from the internet into normal and cancer images with higher accuracy. The Fig.2 is one among those images where the red circle indicates the cancer region of the pancreas.

IV. GRAY SCALE IMAGE

The program converts the colored PET scan images into Gray scale images. The Fig.3 is the Gray scale image of the Fig.2. The gray scale image is used in this work for reducing the computing time of the program.

V. IMAGE DE-NOISING

The Speckle noise is the major noise component present in the medical images [6]. It is a multiplicative noise of random signal whose average amplitude increases with the overall signal intensity. The Speckle noise appears as bright specks in the lighter regions of the image. The mathematical representation of the speckle noise is:

$$I = S + (S \times N_g) \qquad (1)$$

where N_g is the random noise having a zero mean Gaussian probability distributive function. A median filter performs well in removing the Speckle noise from the image [7-8]. The median filter de-noises the image by substituting the actual gray level of a pixel by the median of gray values of pixels in a specific locality. It also preserves the image features like edges while removing the noise. The Fig.4 shows the noise removed image using the median filter.

VI. IMAGE SEGMENTATION

The image segmentation is the process of dividing a digital image into multiple regions and extracting a meaningful region known as the Region of Interest (ROI). The image threshold method is used in this work to extract the cancer region (Region of Interest) from the noised removed image by selecting the Threshold value (T) [9-10]. The expression for the image threshold is:

$$g(x,y) = \begin{cases} 1 \text{ if } f(x,y) > T \\ 0 \text{ if } f(x,y) \leq T \end{cases} \qquad (2)$$

The Fig.5 shows the segmented image in which the white region is the ROI.

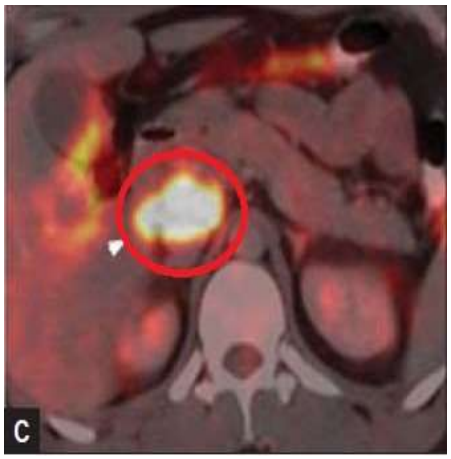

Fig. 2 PET scan image of the pancreas

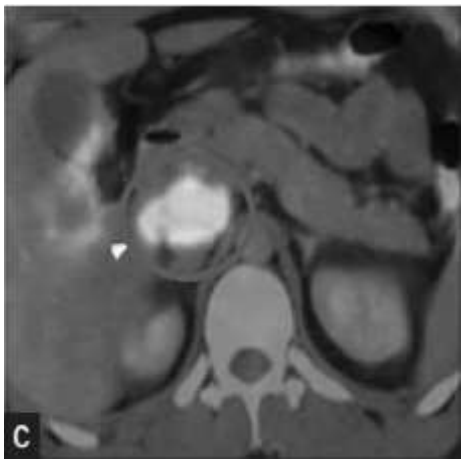

Fig. 3 Gray scale image

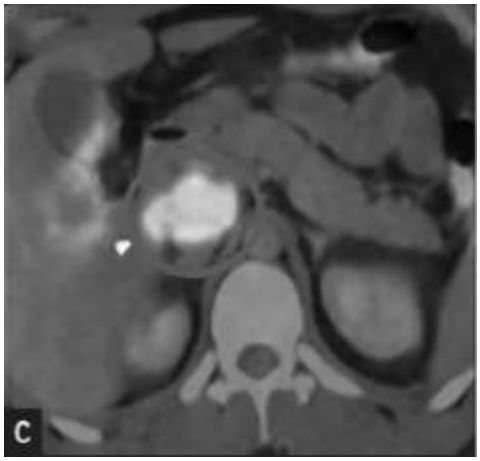

Fig. 4 Noise removed image

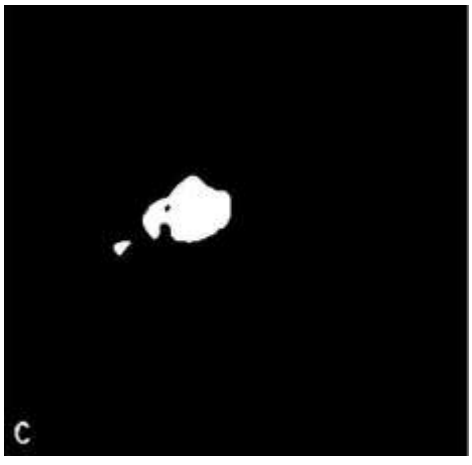

Fig. 5 Segmented image

VII. FEATURE EXTRACTION

A feature is any characteristic or primitive of an object that helps to distinguish or discriminate an object from other objects. The Gray Level Co-occurrence Matrix (GLCM) is a method to extract the texture information of an image. The texture or repeated patterns develop in an image due to variation in the intensity and color of the image. These features are called the Haralick features. The GLCM of an M × N image is a 2D matrix. The elements of this matrix are the joint occurrence of intensity levels X and Y at a certain distance d and an angle θ. In this work, the extracted features using GLCM from the segmented image are Contrast, Correlation, Energy and Homogeneity [11-13]. Table-I provides the extracted features for the first thirty images out of total fifty images.

A. Contrast

It calculates the intensity contrast between a pixel and its neighboring pixel.

$$\text{Contrast} = \sum_{i,j} |i - j|^2 p(i,j) \qquad (3)$$

where $p(i,j)$ is the pixel at the location (i,j)

B. Correlation

The correlation is the measure of linear dependencies of gray levels of the neighboring pixels.

$$\text{Correlation} = \frac{\sum_{i=0}^{N_g-1} \sum_{j=0}^{N_g-1} (i,j) p(i,j) - \mu_x \mu_y}{\sigma_x \sigma_y} \qquad (4)$$

C. Energy

The energy represents the values of the sum of squared elements in the GLCM.

$$\text{Energy} = \sum_{i,j} p(i,j)^2 \qquad (5)$$

D. Homogeneity

The homogeneity is the measure of variation between the elements in a locality.

$$\text{Homogeneity} = \sum_{i,j} \frac{p(i,j)}{1 + |i-j|} \qquad (6)$$

VIII. ANN CLASSIFIER

An Artificial Neural Network resembles a Biological Neural Network with connected

nodes known to be the neurons. The data exchange between the different layers of the neurons takes place by synapses which store the weight to control the data in the calculations. In this work, Multilayer Feed Forward (MLFF) network with Back Propagation (BP) learning is used.

The input-output mapping of MLFF shown in Fig.6 is:

$$O = N_3\left[N_2\left[N_1[I]\right]\right] \quad (7)$$

where the variables N_1, N_2, and N_3 are the non-linear formulations of the input, hidden, and output layers [16].

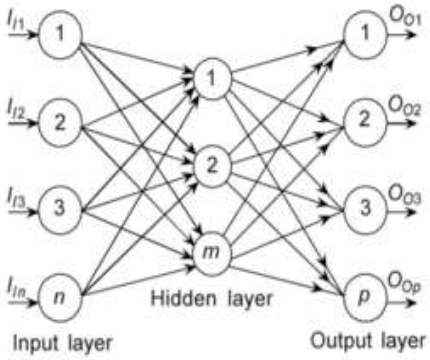

Fig. 6 Multilayer Feed Forward (MLFF) network

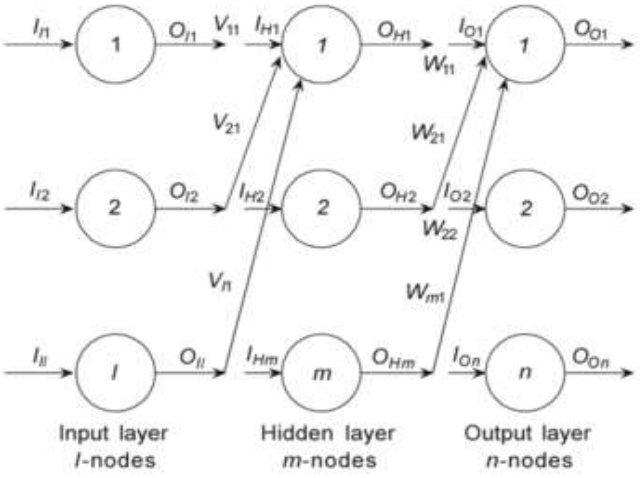

Fig. 7 Multilayer Feed Forward (MLFF) Back Propagation (BP) network

From the Fig.7, the input layer, hidden layer and output layer neurons are computed to be:

The number of input layer neurons is,

$$\{I\}_H = \{V\}^T\{O\}_I \quad (8)$$

where [V] is the weight matrix between the input layer and hidden layer neurons [16

TABLE I. Extracted features using GLCM

Images	Contrast		Correlation		Energy		Homogeneity	
	Min	Max	Min	Max	Min	Max	Min	Max
1	0.0186	0.0191	0.8540	0.8579	0.8506	0.8510	0.9904	0.9907
2	0.0148	0.0153	0.8645	0.8722	0.8698	0.8728	0.9924	0.9926
3	0.0096	0.0102	0.8659	0.8727	0.9142	0.9147	0.9949	0.9952
4	6.2806E-04	7.1998E-04	0.8805	0.8958	0.9933	0.9933	0.9996	0.9997
5	9.1146E-04	9.4975E-04	0.5848	0.6016	0.9968	0.9968	0.9995	0.9995
6	2.5276E-04	3.8297E-04	0.8663	0.7974	0.9979	0.9977	0.9999	0.9998
7	7.7359E-04	0.0011	0.7471	0.6294	0.9962	0.9958	0.9996	0.9994
8	0.0047	0.0056	0.8473	0.8716	0.9575	0.9584	0.9972	0.9976
9	0.0031	0.0041	0.8766	0.9071	0.9624	0.9634	0.9979	0.9984

10	8.2721E-04	0.0017	0.7615	0.8813	0.9914	0.9922	0.9992	0.9996
11	0.0011	0.0013	0.8635	0.8460	0.9906	0.9904	0.9994	0.9994
12	0.0027	0.0032	0.6939	0.6376	0.9886	0.9881	0.9987	0.9984
13	4.2892E-04	9.5741E-04	0.7364	0.8819	0.9954	0.9959	0.9995	0.9998
14	0.0053	0.0085	0.9240	0.9528	0.8796	0.8828	0.9957	0.9974
15	5.8211E-04	0.0045	0.6818	0.9651	0.9826	0.9827	0.9977	0.9997
16	6.6636E-04	6.9700E-04	0.9112	0.9151	0.9915	0.9915	0.9997	0.9997
17	0.0010	0.0013	0.5552	0.6540	0.9957	0.9960	0.9993	0.9995
18	1.3021E-04	1.2255E-04	0.3461	0.3846	0.9997	0.9997	0.9999	0.9999
19	8.7316E-04	8.4252E-04	0.7956	0.8028	0.9949	0.9949	0.9996	0.9996
20	0.0042	0.0047	0.7916	0.7656	0.9758	0.9753	0.9979	0.9977
21	6.5104E-04	0.0011	0.7474	0.5662	0.9968	0.9963	0.9997	0.9994
22	9.1912E-05	1.3787E-04	0.7272	0.5908	0.9996	0.9995	1.0000	0.9999
23	7.0466E-04	8.7316E-04	0.8348	0.7953	0.9950	0.9949	0.9996	0.9996
24	8.1955E-04	7.3529E-04	0.8680	0.8816	0.9930	0.9931	0.9996	0.9996
25	0.0115	0.0166	0.8832	0.9193	0.8417	0.8467	0.9917	0.9943
26	0.0102	0.0122	0.8906	0.8690	0.8966	0.8947	0.9949	0.9939
27	0.0064	0.0085	0.9404	0.9550	0.8491	0.8511	0.9958	0.9968
28	7.7359E-04	0.0010	0.7943	0.7251	0.9955	0.9952	0.9996	0.9995
29	0.0044	0.0050	0.8982	0.9116	0.9457	0.9464	0.9975	0.9978
30	9.4210E-04	0.0013	0.8604	0.8070	0.9923	0.9920	0.9995	0.9993

For sigmoid function, the output of the p^{th} hidden neuron is,

$$O_{Hp} = \frac{1}{\left(1+e^{-\lambda(I_{Hp}-\theta_{Hp})}\right)} \qquad (9)$$

where O_{Hp} is the output of the p^{th} hidden neuron, I_{Hp} is the input of the p^{th} hidden neuron, and θ_{Hp} is the threshold of the p^{th} hidden neuron [16].

For sigmoid function, the output of the q^{th} hidden neuron is,

$$O_{Oq} = \frac{1}{\left(1+e^{-\lambda(I_{Oq}-\theta_{Oq})}\right)} \qquad (10)$$

where O_{Oq} is the output of the q^{th} hidden neuron, I_{Hq} is the input of the q^{th} hidden neuron, and θ_{Hq} is the threshold of the q^{th} hidden neuron [16].

The error function for the training patterns is,

$$E(V,W) = \sum_{j=1}^{nset} E^{j}(V,W,I) \qquad (11)$$

where nset is the pattern set, V and W are the synaptic weights [16].

The ANN classifier used in this work is trained by the contrast and correlation values of the forty images with the target of class ‘0’ for normal images and class ‘1’ for cancer images. The contrast and correlation values of the remaining ten images are given as test images to the classifier with the target of class ‘0’ for normal images and class ‘1’ for cancer images.

IX. EXPERIMENTAL RESULTS AND DISCUSSIONS

The developed ANN based image classifier classified the fifty images into twenty-seven normal images, twenty-two cancer images, and one false negative image.The contingency conditions used in calculating the values of the sensitivity, specificity, and accuracy of the developed diagnosis method using ANN based image classifier are:

- **True Positive (TP) condition:**

This condition implies that both program and radiologist results are positive. It concludes that the diagnosed person has cancer.

- **True Negative (TN) condition:**

This condition implies that both program and radiologist results are negative. It concludes that the diagnosed person does not have cancer.

- **False Positive (FP) condition**:

This condition implies that the program result is positive, and radiologist result is negative which means that the diagnosed person does not have cancer, but the program result shows cancer.

- False Negative (FN) condition:

This condition implies that the program result is negative, and radiologist result is positive which means that the diagnosed person has cancer, and program result shows normal.

Table-II shows the contrast and correlation values of the first thirty images used by the classifier.

The Figs.8, 9, and 10 shows the Performance characteristic, Confusion matrix, and Receiver operating characteristics for the training images of the classifier.

Table-III shows the results of classification performed by the ANN classifier for the first thirty images.

TABLE II. Contrast and Correlation values of the first thirty images used by the classifier

Images	Contrast	Correlation
1	0.0186	0.8550
2	0.0148	0.8650
3	0.0096	0.8720
4	6.2806E-04	0.8810
5	9.1146E-04	0.5850
6	2.5276E-04	0.7980
7	7.7359E-04	0.6295
8	0.0047	0.8474
9	0.0031	0.8767
10	8.2721E-04	0.7620
11	0.0011	0.8636
12	0.0027	0.6940
13	4.2892E-04	0.7365
14	0.0053	0.9242
15	5.8211E-04	0.6820
16	6.6636E-04	0.9113
17	0.0012	0.5553
18	1.3021E-04	0.3462
19	8.7316E-04	0.7957
20	0.0042	0.7657
21	6.5104E-04	0.5663
22	9.1912E-05	0.5910
23	7.0466E-04	0.7954
24	8.1955E-04	0.8820
25	0.0115	0.8833
26	0.0102	0.8693
27	0.0064	0.9406
28	7.7800E-04	0.7252
29	0.0044	0.8983
30	9.4210E-04	0.8073

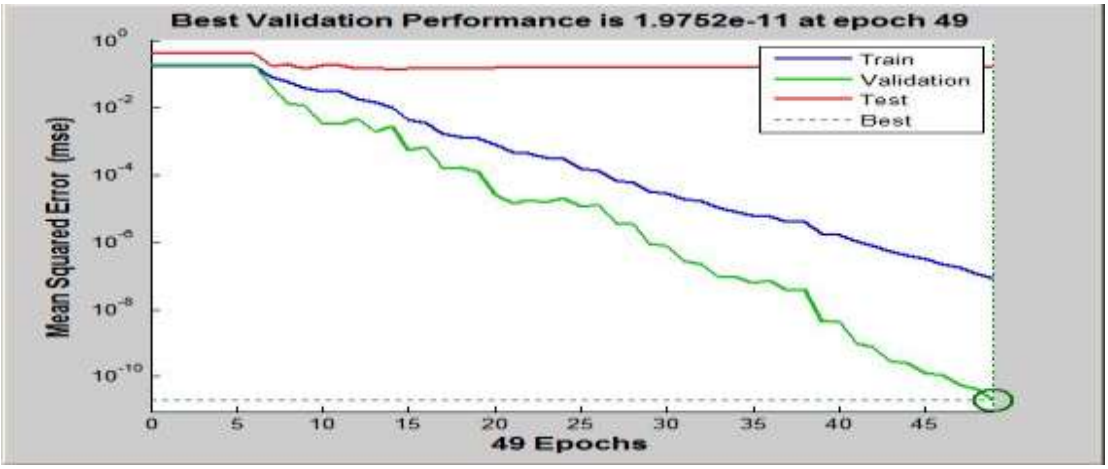

Fig.8 Performance characteristics of the ANN classifier

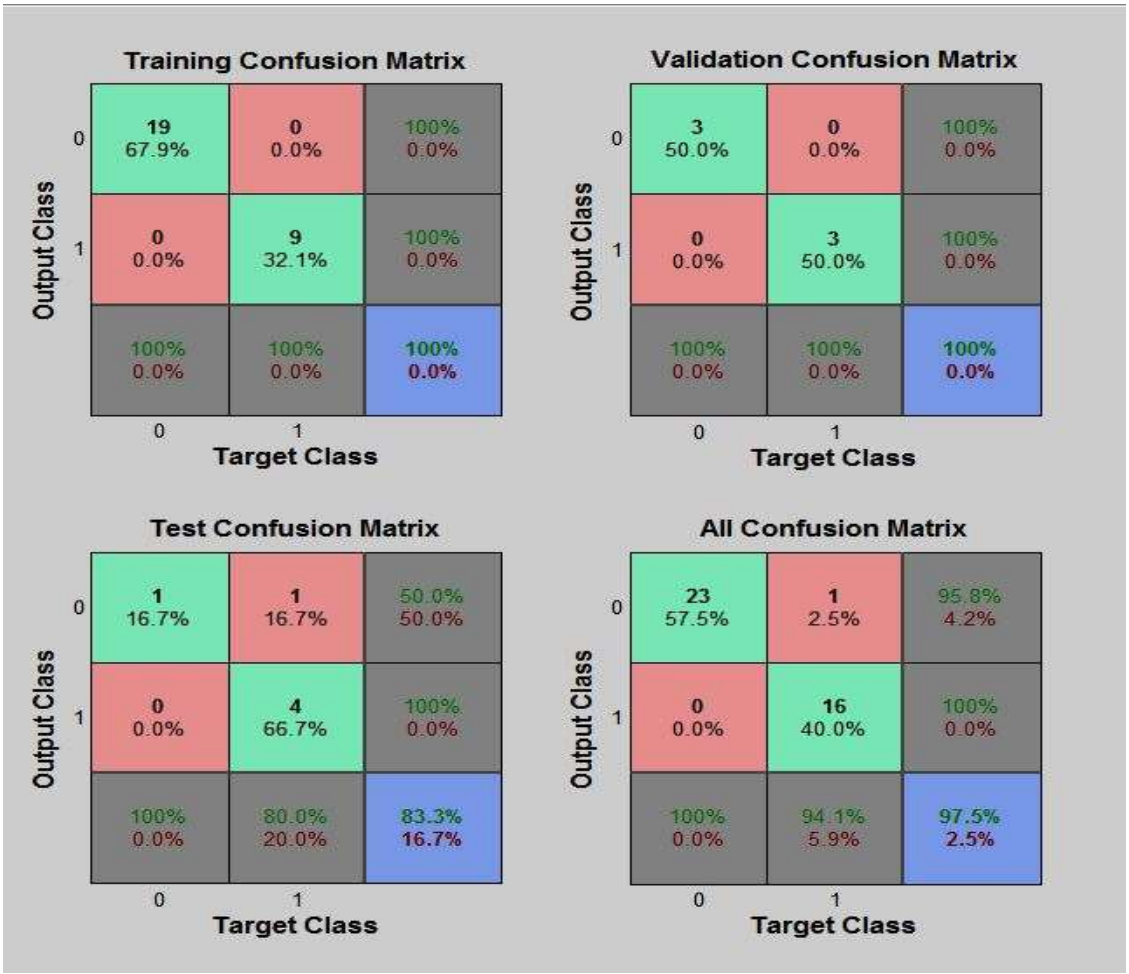

Fig.9 Confusion matrix

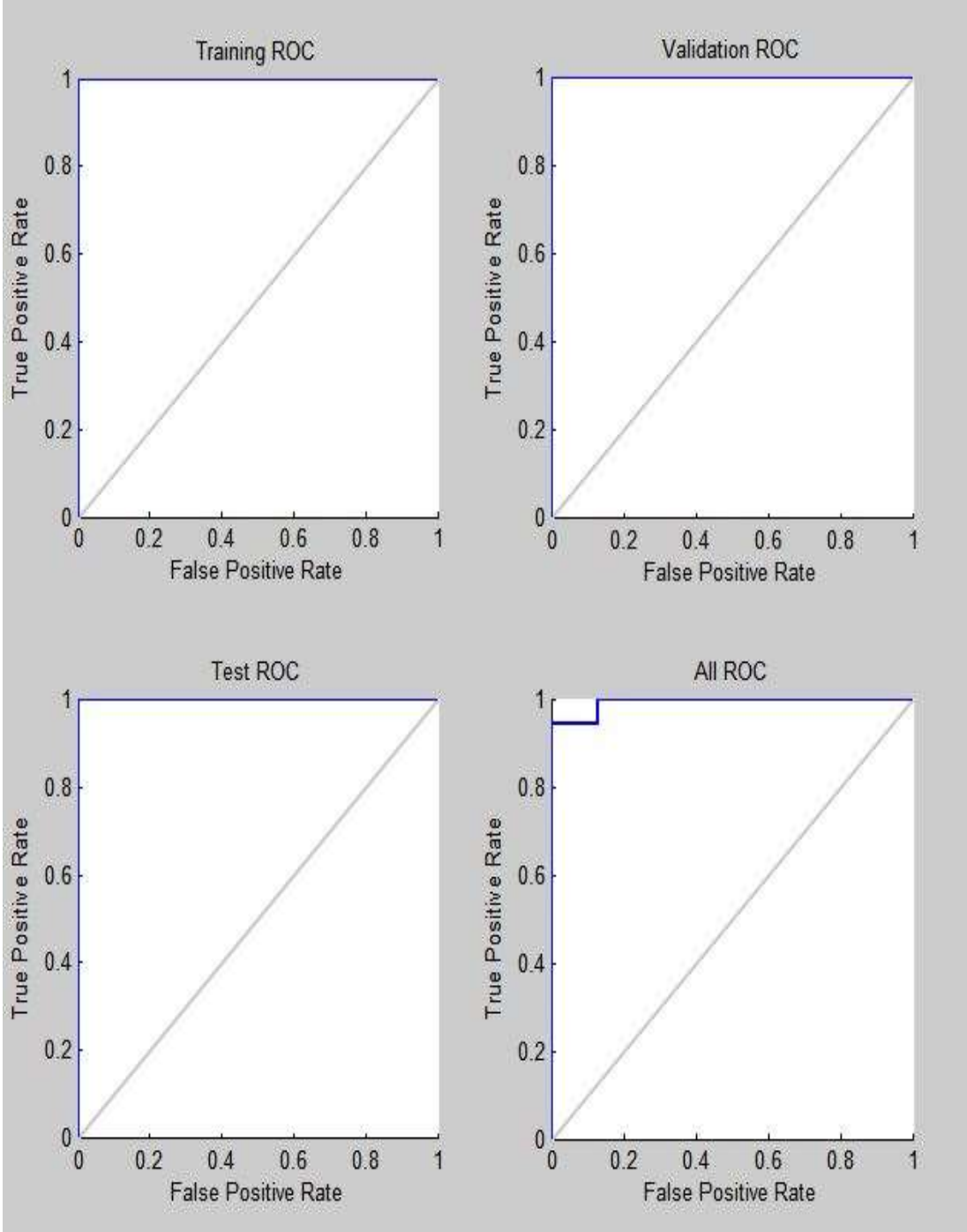

Fig.10 Receiver operating characteristics of the ANN classifier

TABLE III. Results of classification

TP images	TN images	FP images	FN images
22	27	0	1

TP – True Positive, TN – True Negative
FP – False Positive, FN – False Negative

The sensitivity, specificity, and accuracy of the program are calculated from the Table-III by,

A. Sensitivity

The sensitivity is the measure of the proportion of positives that are correctly identified.

Sensitivity = ((TP / (TP + FN)) * 100) % (14)
= 95.65%

B. Specificity

The specificity is the measure of the proportion of negatives that are correctly identified.

Specificity= ((TN/ (TN + FP)) * 100) % (15)
= 100%

C. Accuracy

The accuracy is the measure of the degree of closeness of measurements of a quantity to that quantity's true value.

Accuracy=
((TP+TN)/(TP+TN+FP+FN))*100)% (16)
= 98%

D. Comparison with the existing method

The developed method of pancreatic cancer detection using image processing with ANN classifier provides an accuracy of 98% which is higher than the existing method of pancreatic cancer detection by CT scan images and minimum-distance classifier, for which the accuracy obtained, is of 65.26%. Also, the sensitivity of the proposed method is high (95.65%) i.e. out of fifty images the program correctly identifies forty-nine images.

X. CONCLUSION

The developed ANN based image classifier detects pancreatic cancer at the early stage with very high accuracy of 98%. The major advantages of using this method for pancreatic cancer detection are: the cancer detection does not rely on the radiologist experience which is a major drawback in Abdominal Ultrasonography, it provides information about staging which is not visible in the MRI scan and it can detect even a small-sized tumor which the CT or MRI scans fails to capture. This method does not cause any infection to the pancreas during the diagnosis, but in the case of an Endoscopic Ultrasonography, there is a chance of causing infection and inflammation to the pancreas. In most of the pancreatic cancer cases, the survival rate of the patients mainly depends on the early detection of the disease. The ANN based image classifier will improve the survival rate of those patients as it is capable of detecting the disease at the early stage. The experimental results of sensitivity, specificity, and accuracy of this method are 95.65%, 100%, and 98%.

XI. REFERENCES

[1] 'World Cancer Research Fund International', http://www.wcrf.org/int/cancer-facts figures/data-specific-cancers/pancreatic-cancer-statistics, accessed 11 October 2015.
[2] American Cancer Society, 'Cancer Facts and Figures Report 2015', pp. 19 – 20.
[3] 'Pancreatic cancer patients in India', http://www.pancreaticcancerindia.com/files /hp/incidence.html, accessed 11 October 2015.
[4] Andrea Gallamini, Colette Zwarthoed, Anna Borra: 'Positron Emission

Tomography (PET) in Oncology', MDPI Journal, 2014, 6, pp 1821 – 1822.

[5] Jeenal Shah, Sunil Surve, Varsha Turkar: 'Pancreatic Tumor Detection using Image processing', Proc. 4th International Conference on Advances in Computing, Communication and Control, Mumbai, India, April 2015, pp 1-16.

[6] Sridhar.S: 'Digital Image Processing', (Oxford University Press, first published 2011), pp 220 & 320.

[7] Gopinathan S, Poornima S: 'Enhancement of images with speckle noise reduction using different filters', Int. Journal of Applied Sciences and Engineering Research, 2015, 4(3), pp 334 & 336.

[8] Mr. Rohit Verma and Dr. Jahid Ali: 'A comparative study of various types of image noise and efficient noise removal techniques', International Journal of Advanced Research in Computer Science and Software Engineering, 2013, 3(10), pp 622.

[9] Rozy Kumari, Narinder Sharma: 'A Study on the Different Image Segmentation Technique', International Journal of Engineering and Innovative Technology (IJEIT), 2014, pp 285 – 286.

[10] Swati Matta: 'Review: Various Image Segmentation Techniques', International Journal of Computer Science and Information Technologies, 2014, 5(6), pp 7537.

[11] Minakshi Sharma, Sourabh Mukherjee: 'Brain Tumor Segmentation using hybrid Genetic Algorithm and Artificial Neural Network Fuzzy Inference System (ANFIS)', International Journal of Fuzzy Logic Systems (IJFLS), 2012, 2(4), pp 35-36.

[12] Mohanaiah. P, Sathyanarayana. P, Guru Kumar. L: 'Image texture feature extraction using GLCM approach', International Journal of Scientific and Research Publications, 2013, 3(5), pp 1-2.

[13] Pauline John: 'Brain Tumor Classification Using Wavelet and Texture-Based Neural Network', International Journal of Scientific & Engineering Research, 2012, 3(10), pp 3-4.

[14] Alireza Osareh, Bita Shadgar: 'Machine Learning Techniques to Diagnose Breast Cancer', IEEE, 2010, pp 116 -119.

[15] Pavan Tummala, Omer Junaidi, Banke Agarwal: 'Imaging of pancreatic cancer: An overview', Journal of Gastrointestinal Oncology, 2011, pp 168-174.

[16] Rajasekaran. S, Vijayalakshmi Pai. G.A.: 'Neural Networks, Fuzzy Logic, and Genetic Algorithms – Synthesis and Applications', (PHI Private Limited, Twelfth print 2009), pp 41-56.

[17] 'Artificial neural Network', http://in.mathworks.com/help/nnet/gs/classify-patterns-with-a-neural-network.html, accessed 12 February 2016.

[18] 'Artificial neural Network', http://in.mathworks.com/help/nnet/ug/configure-neural-network-inputs-and-outputs.html, accessed 12 February 2016.

[19] 'Artificial neural Network', http://in.mathworks.com/help/nnet/ref/train.html, accessed 12 February 2016.